

Evaluation of Hot Corrosion Behavior of APS and HVOF Sprayed Thermal Barrier Coatings (TBCs) Exposed to Molten $\text{Na}_2\text{SO}_4 + \text{V}_2\text{O}_5$ Salt at $1000\text{ }^\circ\text{C}$



Mustafa Kaplan, Mesut Uyaner, Yasin Ozgurluk, Kadir Mert Doleker and Abdullah Cahit Karaoglanli

Abstract Hot corrosion is a very destructive failure mechanism for thermal barrier coatings (TBCs) during service conditions. In the present study, a CoNiCrAlY is coated using atmospheric plasma spray (APS) and high velocity oxy-fuel (HVOF) techniques which produces TBCs that were exposed to 50% Na_2SO_4 and 50% V_2O_5 molten salts at $1000\text{ }^\circ\text{C}$. The top surface was visually inspected at the end of each four-hour cycle to determine the lifetime of TBCs. The failure criteria required for the termination of the hot corrosion cycles was assumed to be 25% cracking and spallation of top coats. X-Ray Diffraction (XRD) analysis was performed before and after hot corrosion tests in order to observe new phases which may occur in the top coating. After scanning electron microscopy (SEM) images of cross-section samples of hot corrosion tests are completed, samples were taken. As a result, it has been observed that the lifetimes of HVOF bond-coated TBCs are longer.

Keywords Thermal barrier coatings (TBCs) · Atmospheric plasma spray (APS) · High velocity oxy-fuel (HVOF) · Hot corrosion · $\text{Na}_2\text{SO}_4 + \text{V}_2\text{O}_5$ salt

M. Kaplan

Department of Metallurgical and Materials Engineering, Graduate School of Natural and Applied Sciences, Selcuk University, 42003 Konya, Turkey
e-mail: mkaplan5442@gmail.com

M. Uyaner

Department of Aeronautical Engineering, Faculty of Aeronautics and Astronautics, Necmettin Erbakan University, 42090 Konya, Turkey
e-mail: muyaner@konya.edu.tr

Y. Ozgurluk (✉) · K. M. Doleker · A. C. Karaoglanli
Department of Metallurgical and Materials Engineering,
Bartın University, 74100 Bartın, Turkey
e-mail: ozgurlukyasin@gmail.com

K. M. Doleker

e-mail: mertdoleker@gmail.com

A. C. Karaoglanli

e-mail: cahitkaraoglanli@gmail.com

1 Introduction

Thermal barrier coatings (TBCs) are widely used to provide thermal insulation to the hot section components of gas turbines and aero engines in order to protect them from thermal degradation and also increase efficiency and durability properties of these components [1–3]. A typical TBC consists of a superalloy substrate that a MCrAlY bond coat is applied onto together with a ceramic top coat of 6–8 wt% yttria partially stabilized zirconia (YSZ). The bond coating provides high temperature oxidation and corrosion resistance, while the top coat offers thermal insulation at high operating temperatures. Many factors influence the lifetime of TBCs during service. Among them, the strength of the bond coat layer against failures such as oxidation and hot corrosion is the critical role of this layer in TBCs. When the TBC is exposed by oxidation with high temperature, oxide formation occurs at the top coat and bond coat interface which is called a thermally grown oxide (TGO) [1, 4–6].

A TGO is formed during the partial deposition of however it usually starts to grow due to the high temperature oxidation between bond coat and ceramic top coat. After that the TGO leads to spallation of the top coat from the bond coat. In TBC systems, spallation arising from TGO is observed as the most common failure. Thus, the growth of TGO leads to degradation and failure of the coating. Furthermore, the thermal expansion mismatch between the bond coat and the ceramic topcoat causes the coating to fail during cooling and heating. The ceramic top coat has a low thermal conductivity and partially low thermal expansion. The metallic bond coats are deposited between the metallic substrate and ceramic top coat for improving adhesion [4, 7, 8].

Another failure mechanism in TBC systems are the one that occur from topcoat phase transformation. Phase transformation and cracking of the top coat has a major impact on the lifetime of the TBCs. At higher operation temperatures, the ceramic top coat undergoes phase transformation from a tetragonal to monoclinic form.

In this study, Atmospheric Plasma Spray (APS) and High Velocity Oxy-Fuel (HVOF) techniques have been used to deposit CoNiCrAlY based metallic bond coats on nickel-based Inconel 718 superalloy substrates. The APS method was only used for deposition of ceramic top coatings with YSZ content. The main purpose of the study is the evaluation of failure mechanisms and lifetime of TBC systems produced by using bond coatings applied by APS and HVOF methods under high temperature and hot corrosion conditions.

2 Experimental Methods

2.1 Preparation of Substrate Material, Bond and Top Coatings

The substrates were cut into disks with 1 inch diameters and 4 mm thickness, from a wrought sheet of nickel based superalloy. The substrate surfaces were subject to an ultrasonic cleaning and grit blasting process in order to improve the adherence of the coating. Commercial CoNiCrAlY bond coating (Sulzer-Metco, USA, Amdry 9951, 5–37 μm) and ZrO₂-8 wt% Y₂O₃ top coating (GTV Germany, –45 to +20 μm) powders were deposited on nickel based superalloy substrates. The thickness of the bond and the ceramic top coat are 100 μm and 300 μm , respectively.

2.2 Hot Corrosion Tests

In this study, the 99% purified Na₂SO₄ and 98% purified V₂O₅ salt mixtures with a mass ratio of 1:1 was selected as the corrosive salt. The corrosive salt was first spread on the surface of the produced TBC samples uniformly with a salt amount of 10 mg/cm². This process was repeated at the beginning of each cycle. After that, prepared specimens are subjected to hot corrosion tests at a temperature of 1000 °C with the periodical cycle of four hours. And then the samples were removed from the furnace and cooled down to room temperature. Hot corrosion tests are continued until approximately 25% degradation of the samples was observed.

2.3 Characterization

Microstructures of whole TBCs produced in this study are examined via scanning electron microscopy (SEM, Tescan, MAIA3 XMU, Czech Republic) equipped with energy dispersive spectroscopy (EDS; Oxford Xmax 50, Britain). The content of coats was determined by X-ray diffraction (Rigaku Dmax 2200 PC, Cu Ka radiation, Rigaku, Japan). Surface and cross-sectional microstructural analysis, and phase transformations were carried out to examine corrosive product formation and degradation mechanisms. Some important findings were presented.

3 Results and Discussion

3.1 Characterization of as-Sprayed Coatings

In this study, APS and HVOF techniques were used in the production of TBC systems. While metallic bond coats were produced by the APS and HVOF methods, top coat YSZ was produced only by APS method. As-sprayed surface image of YSZ TBC produced by APS method is shown in Fig. 1. The ceramic top coat, which typically consists of APS-deposited TBCs, has roughness and cracks. As a result of this, the oxygen penetration to YSZ top coat layer is high. The combination of all the conditions leads to the oxidation of the TBCs and the formation of TGO at the bond and top coat interface. At the same time, different corrosive salts and pollutions, which are results of the burning of low-quality fuels, after suffering corrosive penetration through the top coat of TBCs can be cause a damage [5, 8–10].

The microstructure of TBC coatings which is produced using the APS technique contains intense amounts of porous and oxide depending on the production process

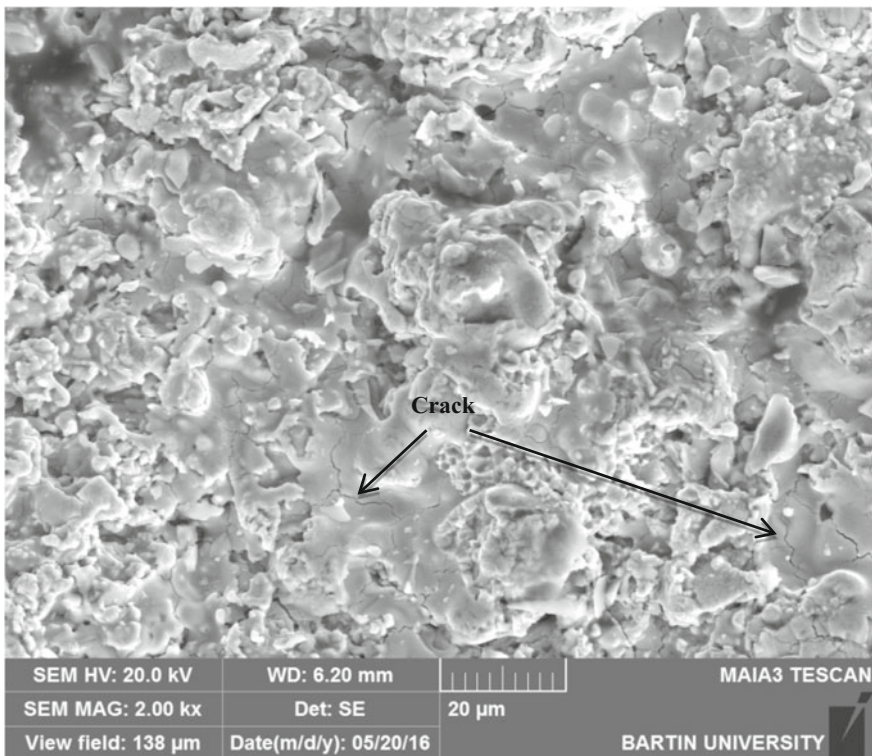


Fig. 1 As-sprayed surface image of YSZ TBC produced by APS method

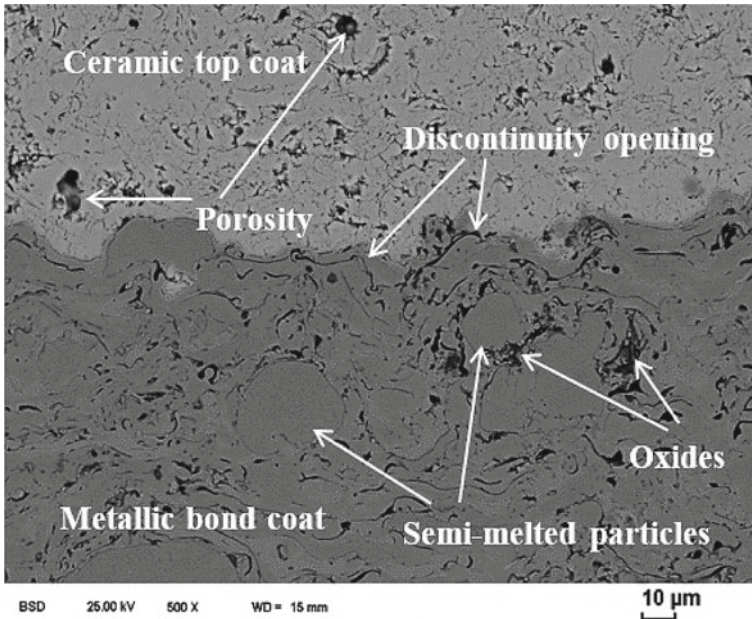


Fig. 2 As-sprayed cross-sectional microstructure of YSZ TBC and CoNiCrAlY bond coat produced with APS method

and spraying condition. This is also a consequence of the fact that the process is carried out open to the atmosphere. The as-sprayed cross-sectional microstructure of YSZ TBCs and CoNiCrAlY bond coatings produced using the APS method is shown in Fig. 2. The metallic bond and ceramic top coat, which was produced by APS methods, had porosities, cracks, discontinuity openings, and oxides. Besides, some melted or semi-melted particles were observed, which is caused by high velocity spraying and the high melting points of the powders. As previously mentioned, the microstructure of the APS coating contains pores and micro-cracks, which is emphasized in the literature on produced by APS technique with YSZ containing coating studies [11–15]. An as-sprayed cross-sectional micrograph of YSZ TBCs produced using by APS method with HVOF CoNiCrAlY bond coat is shown in Fig. 3. When as-sprayed TBCs were evaluated, microstructures of TBCs produced by using APS method have porosity, cracks and discontinuous openings whereas microstructures of TBC produced by the HVOF method have less porosity and content of oxide.

3.2 Hot Corrosion Effect on TBC Samples

It is known that low-quality fuels containing impurities at a high rate (S, V, Na, Ca, K and P) promote hot corrosion depending on the failures in the combustion chambers

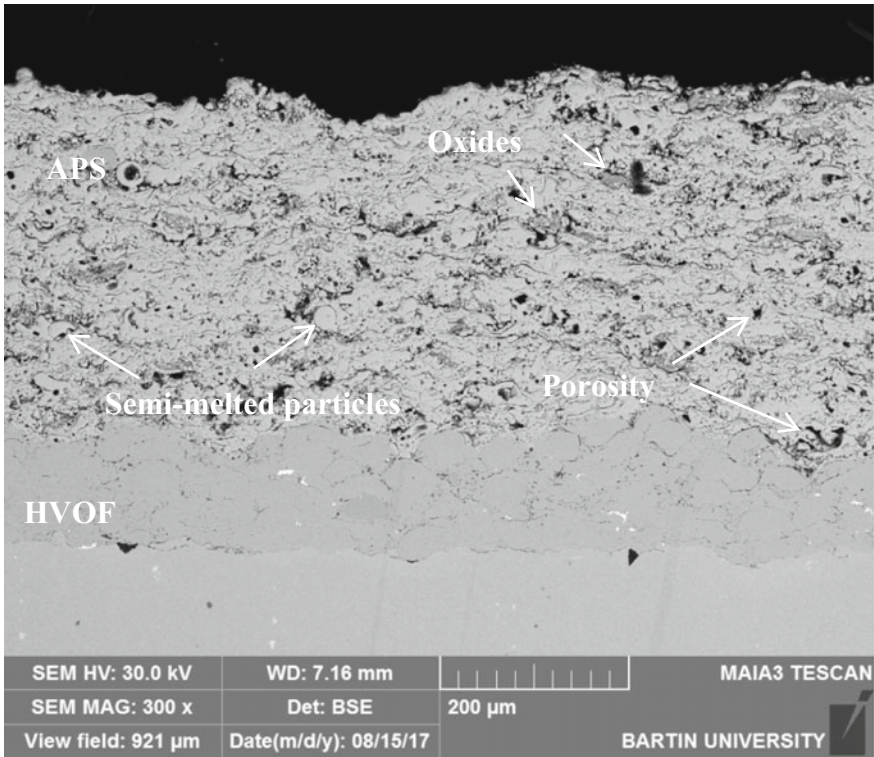


Fig. 3 As-sprayed cross-sectional micrograph of YSZ TBC produced by APS method with HVOF CoNiCrAlY bond coat

of gas turbine components. Hot corrosion happens as a result of melted corrosive salts leaking from micro-cracks or porosities on the top coat layer. The top coat has a roughness structure and microcracks (Fig. 1). Thus, it increases the interactions of corrosive salts on the top coat layer. A study by Sreedhar et al. supports this idea [1]. At the same time, repeated melting/solidification cycles of these corrosive salts deposited on the coating at elevated temperatures cause the degradation of the TBC components. In addition, they directly have chemical interaction with yttria (Y_2O_3) which contains $t\text{-ZrO}_2$ phases. This interaction is accelerated by the degradation of TBCs, especially the degradation of the semi-stable structure of the top ceramic (YSZ) coating, the formation of the TGO ($\alpha\text{-Al}_2O_3$) structure, the damage of the metallic bond coating, and the hot corrosion of the superalloy substrate material. Hot corrosion tests were carried out at a temperature of 1000 °C to exceed the melting temperatures of the corrosive salts. Thus, the complete dissolution of the corrosive salts and the interactions with top coat has been achieved [16]. It was found that the corrosive salts primarily react with yttria, the stabilizer of YSZ, which degrades the stable structure of YSZ. Therefore, as the yttria elements are consumed in the structure, the process of $t\text{-ZrO}_2$ to $m\text{-ZrO}_2$ transformation occurs. This phase

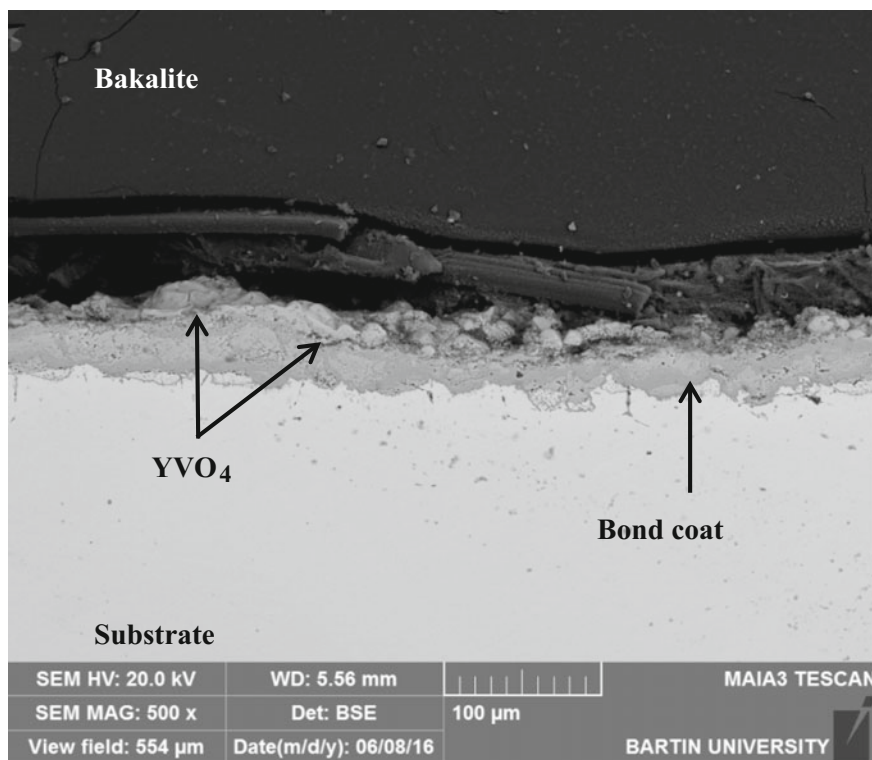


Fig. 4 Cross-sectional micrograph of YSZ TBC and CoNiCrAlY bond coat produced by APS method after the hot corrosion test

transformation causes approximately 3–5% volume expansion of the top coating. Following this, it leads to cracking and spallation of the YSZ coating [9]. In addition, many studies have shown that molten corrosive salts such as Na_2SO_4 and V_2O_5 are completely penetrated by the YSZ top coating at this temperature [5, 17].

A cross-sectional micrograph of the YSZ TBCs and CoNiCrAlY bond coatings produced by the APS method after hot corrosion testing is shown in Fig. 4. As a result of a total of 12 cycles of hot corrosion tests carried out in the 4 h cycle, TBCs failed by spallation from the top coat/bond coat interface. The reason for the spallation of the top coat from the bond coat is the penetration of oxygen through the bond and ceramic coating interface during hot corrosion. Spallation symptoms and cracks were observed on the surface area of coatings from the edge to the center at the end of each cycle. Besides, an YVO_4 corrosion product is observed in Fig. 4. A similar mechanism of failure has also been mentioned in earlier reports. In addition, it has been suggested that the mixed oxides formed in the TGO build up the stress in the structure and accelerate the formation of failure [9, 18–20].

A top surface micrograph of the YSZ and CoNiCrAlY bond coating produced by APS after the hot corrosion test is shown in Fig. 5. After the corrosion test conducted

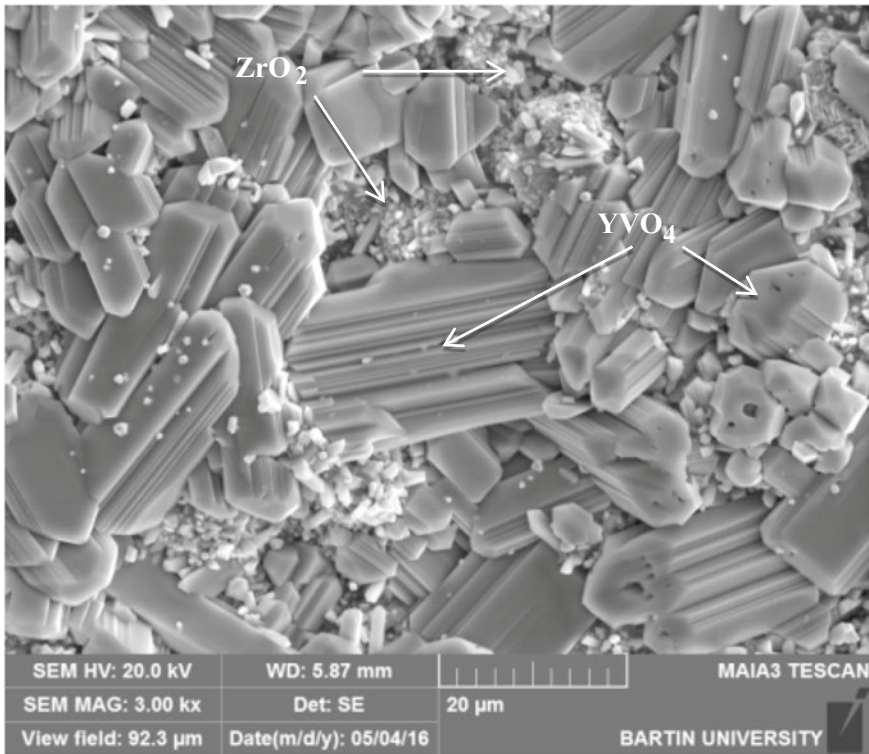


Fig. 5 Top surface micrograph of YSZ TBC and CoNiCrAlY bond coat produced by APS after the hot corrosion test

at 1000 °C for a period of 48 h, the majority of YSZ coating surfaces were coated with corrosion products. Besides, phase transformations occurred with the impact of $\text{Na}_2\text{SO}_4 + \text{V}_2\text{O}_5$ molten corrosive salts.

Top surfaces micrographs of the YSZ TBCs and CoNiCrAlY bond coatings produced by APS after the hot corrosion test for (a) 12 h, (b) 24 h, (c) 36 h and (d) 48 h are illustrated in Figs. 5 and 6, YVO_4 rod crystals are observed on the surface of YSZ coatings during the hot corrosion investigation. In the figures ZrO_2 is also shown. It has been observed that the corrosion products (YVO_4) were crystallized to form rod shaped and irregular crystals, especially in the void areas of the coating surface. As the number of hot corrosion cycles increases, corrosion products are more dominant on the coating surface. It was reported that the corrosion product also increases parallel with the increasing number of cycles in the study conducted by Guo et al. [17].

A surface micrograph with EDS analysis of YSZ TBCs and CoNiCrAlY bond coatings produced by the APS method after the hot corrosion test is given in Fig. 7. In the figure, the rod-shaped structures are found by EDS analyses. The rod-shaped structures were formed as YVO_4 after the hot corrosion test. Besides the vanadate

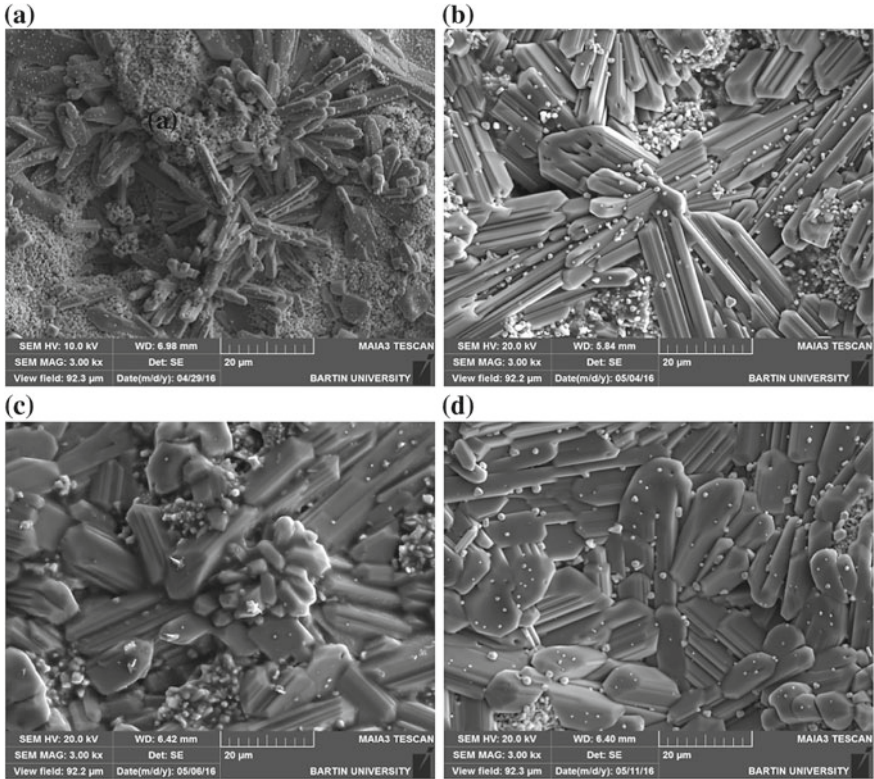
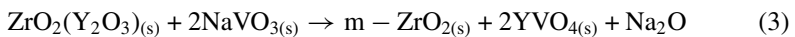
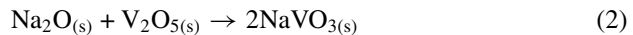
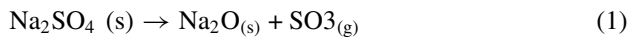


Fig. 6 Top surfaces micrograph of YSZ and CoNiCrAlY bond coat produced by APS after the hot corrosion test for **a** 12 h, **b** 24 h, **c** 36 h and **d** 48 h

corrosion product, the $m\text{-ZrO}_2$ phase was also detected. Initially with increasing temperature, Na_2SO_4 did not show any chemical reaction directly on YSZ. However, with the Na_2SO_4 corrosive salt present in the environment, $\text{SO}_3(g)$ reacts with Y_2O_3 under relative partial pressure to deteriorate the stable structure of YSZ. When Y_2O_3 is absent, a tetragonal to monoclinic phase transformation happens and the stabilization of the tetragonal ZrO_2 phase is lost. The integrity of the structure is destroyed due to the transformation [13, 18, 21, 22].

It is thought that Y_2O_3 , which is a stabilizer for the transformation of ZrO_2 to the semi-stable form, occurs after the interaction. As a result, SO_3 and the other melt precipitators accelerated the mechanism of destruction. The reactions occurred during the hot corrosion process are as follows.



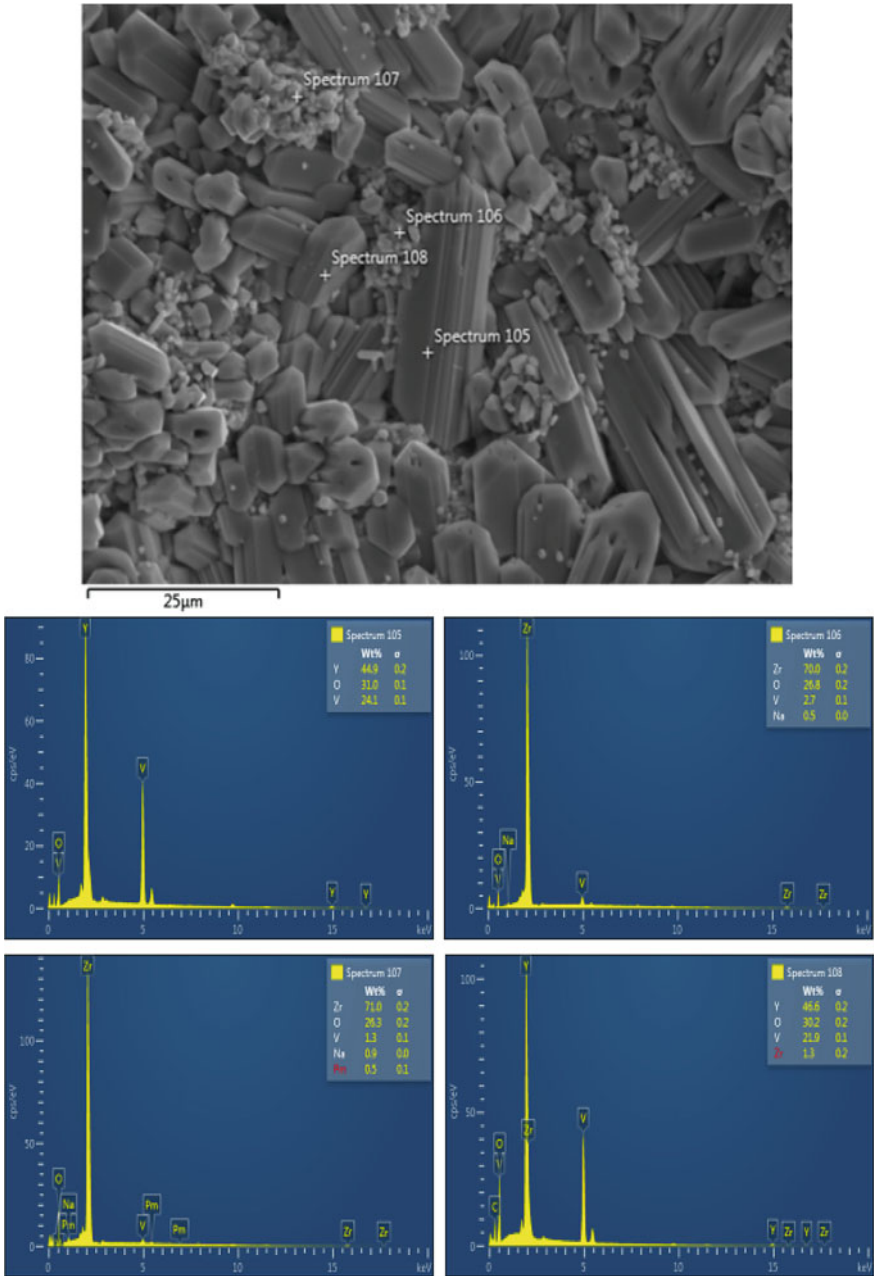


Fig. 7 Surface micrograph with EDS analysis of YSZ TBC and CoNiCrAlY bond coat produced by APS method after the hot corrosion test

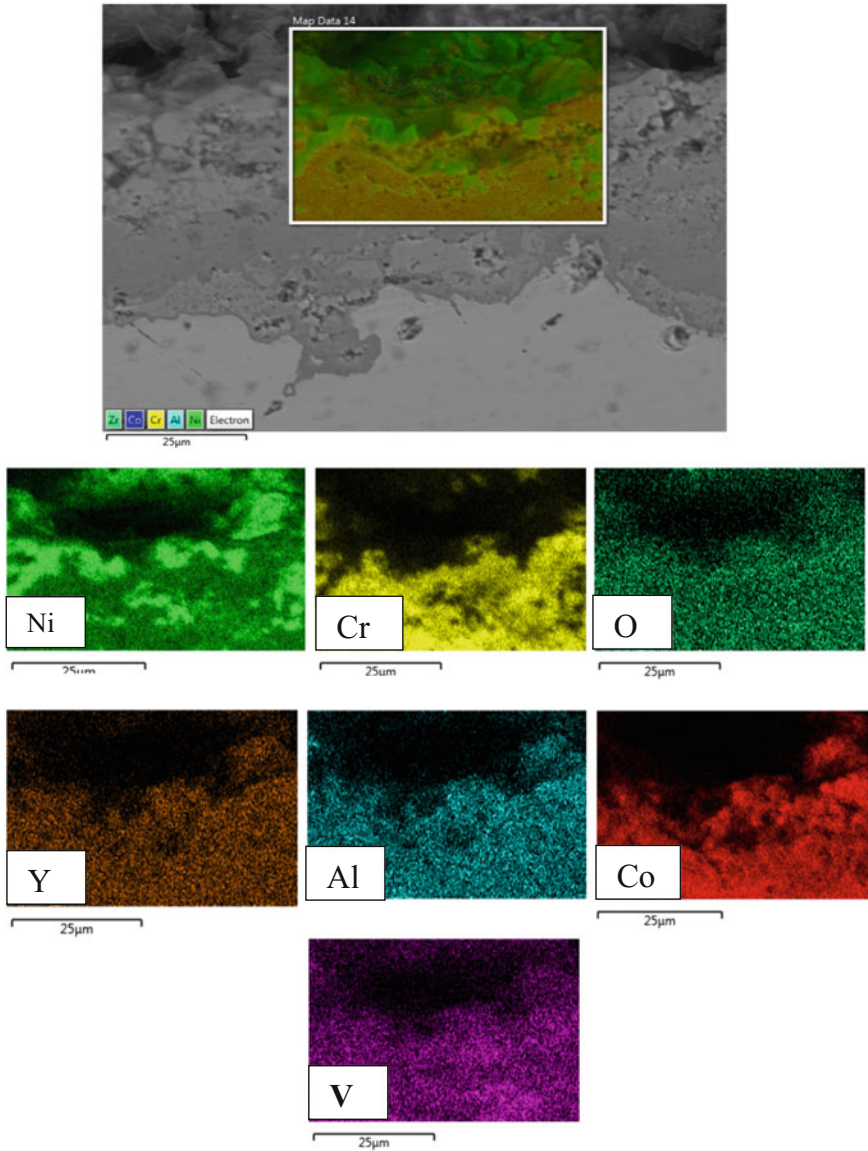


Fig. 8 Cross-sectional micrograph with elemental mapping analysis of YSZ TBC and CoNiCrAlY bond coat produced by APS method after the hot corrosion test

During the process of hot corrosion on YSZ, yttria elements gradually run out. After that, tetragonal zirconia loses semi-stable form and transforms to monoclinic zirconia. The below reaction can also occur [5, 19, 23].

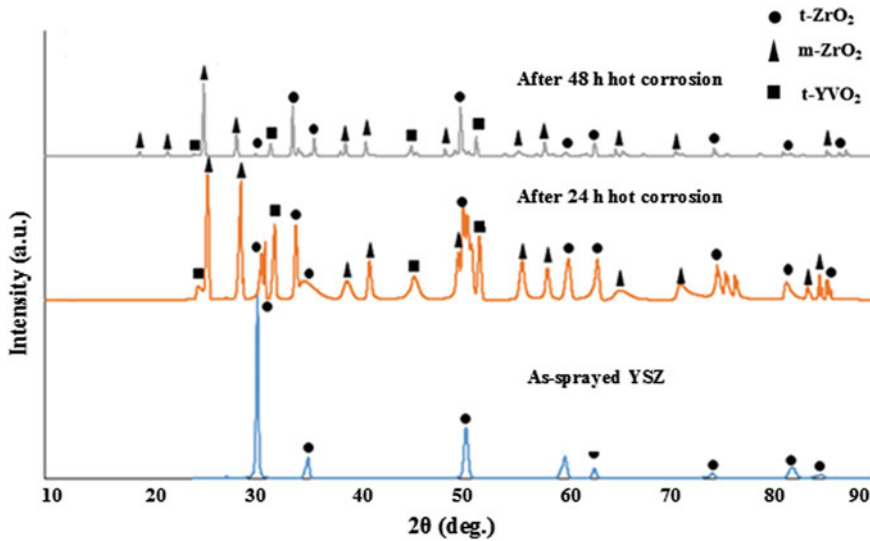
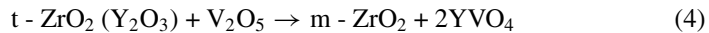


Fig. 9 XRD analysis of YSZ TBC and CoNiCrAlY bond coat produced by APS before and after hot corrosion tests



A cross-sectional micrograph with elemental mapping analysis of YSZ TBCs and CoNiCrAlY bond coatings produced by the APS method after the hot corrosion test is demonstrated in Fig. 8. The elemental mapping analysis after hot corrosion testing can be shown in Fig. 8 hot corrosion products. It can be understood from the elemental mapping analysis that one of the hot corrosion products is YVO_4 rod-shaped crystals.

The XRD analysis of YSZ TBC and CoNiCrAlY bond coat produced by APS before and after hot corrosion tests is given in Fig. 9. Tetragonal ZrO_2 is only encountered on the top coating before hot corrosion. However, the XRD analysis showed that phases of YVO_4 , $m\text{-ZrO}_2$ and $t\text{-ZrO}_2$, occurred in the coat after hot corrosion. Therefore, the top coat caused deterioration by phase transformations. With regard to the patterns of the as-sprayed TBC samples most of the tetragonal zirconia in the YSZ has transformed to the monoclinic phase and YVO_4 which is the hot corrosion product. So, hot corrosion leads to phase transformation on the top coating. This phase transformation generally disrupts the function of the top coat [4, 9, 24].

A cross-sectional micrograph of TBC produced by APS method with HVOF CoNiCrAlY bond coating after hot corrosion at 1000 °C for 52 h is illustrated in Fig. 10. Primarily, it is observed that TGO formed along the interface of the bond coat and top coat layer which includes mixed oxides under the hot corrosion. Besides, cracks are formed as vertical to the interface TGO/top coat. In addition, the HVOF TBCs exposed to hot corrosion salts exhibited spallation of the top coat at near the bond coat/top coat interface. In similar studies conducted with YSZ top coating in

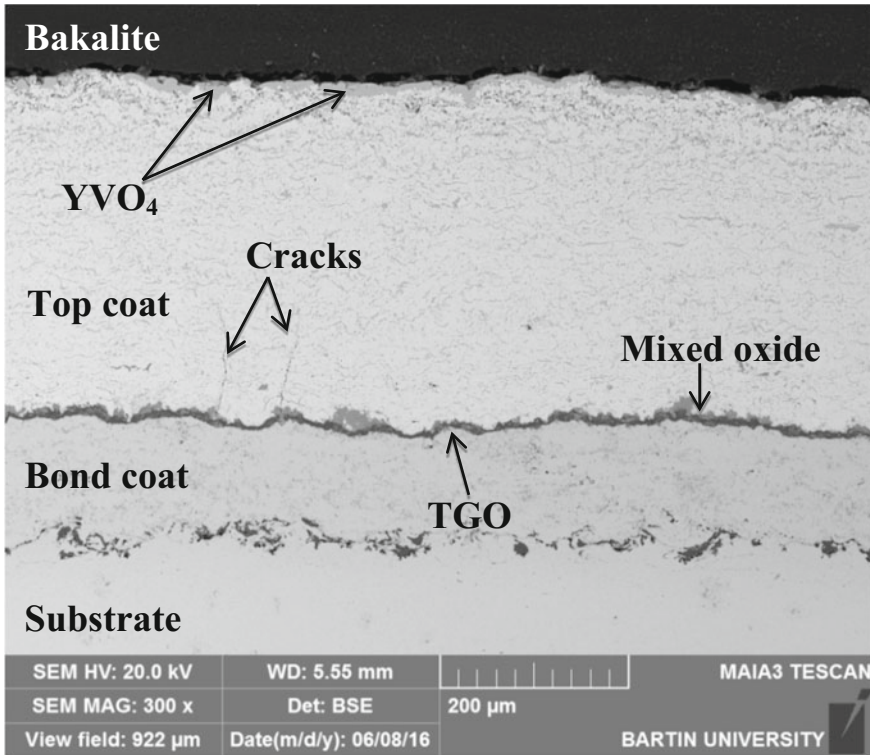


Fig. 10 Cross-sectional micrograph of YSZ TBC produced by APS method with HVOF CoNiCrAlY bond coat after the hot corrosion test

Na₂SO₄ and V₂O₅V, mixture molten corrosive salts were observed on top coatings of TBC systems. Moreover, it was reported that spallation and phase transformation occurs in the top coatings in the studies [9, 25, 26].

APS TBCs with HVOF sprayed CoNiCrAlY bond coating surface SEM images and EDS analysis after 52 h hot corrosion test are shown in Figs. 11 and 12, respectively. The observation of the surface morphology of the coating showed that the corrosion product, which is YVO₄ rod-shaped crystals after the 52 h cyclic hot corrosion test is shown in Fig. 12. These formations have been observed in similar studies in the literature [27, 28]. As shown in Fig. 12, the elements yttria were detected by EDS on surfaces of rod-shaped crystals. So, vanadium may form compounds as vanadate during hot corrosion [27]. Besides, the formation of YVO₄ was confirmed using the EDS analysis in this figure.

Cross-sectional micrographs with elemental mapping analysis of YSZ TBC produced by the APS method with HVOF CoNiCrAlY bond coating after the hot corrosion test is demonstrated in Fig. 13. The corrosion product components can be easily observed by elemental mapping analysis after the hot corrosion test. Besides, oxygen coinciding with the vanadium and yttria elements are shown. In addition to

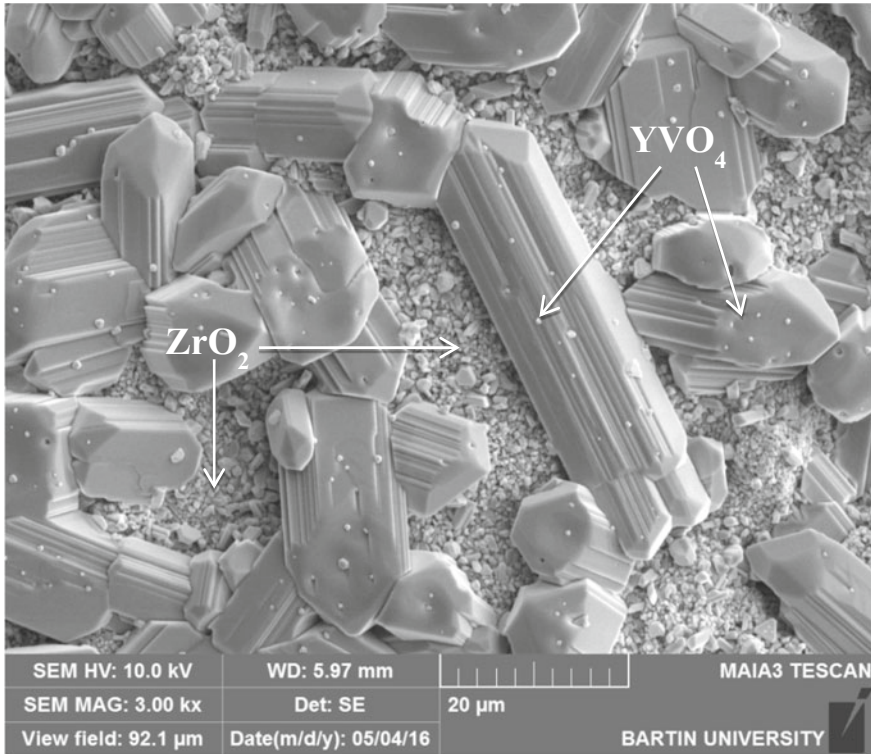


Fig. 11 Surface micrograph of YSZ TBC produced by APS method with HVOF CoNiCrAlY bond coat after the hot corrosion test

the corrosion products, it can be understood that aluminum has been joined to the TGO structure. In addition to EDS and elemental mapping analyses, XRD phase analysis shows an YVO_4 phase, and another hot corrosion product, namely monoclinic ZrO_2 , as shown in Figs. 9 and 14. The XRD analysis of the hot corroded YSZ top coating shown in Figs. 9 and 14 confirms the formation of the YVO_4 phase. Figures 9 and 14, the presence of a few tetragonal zirconia phases can be seen, while more number of zirconia monoclinic phases indicating the extensive destabilization of YSZ coating and also TBC system after 52 h hot corrosion testing. Ramachandran et al. [27] reported the presence of the phases.

4 Conclusion

In the present study, the hot corrosion behavior of the two different TBC systems including a CoNiCrAlY bond coat and an YSZ top coat have been compared. The following conclusions are drawn:

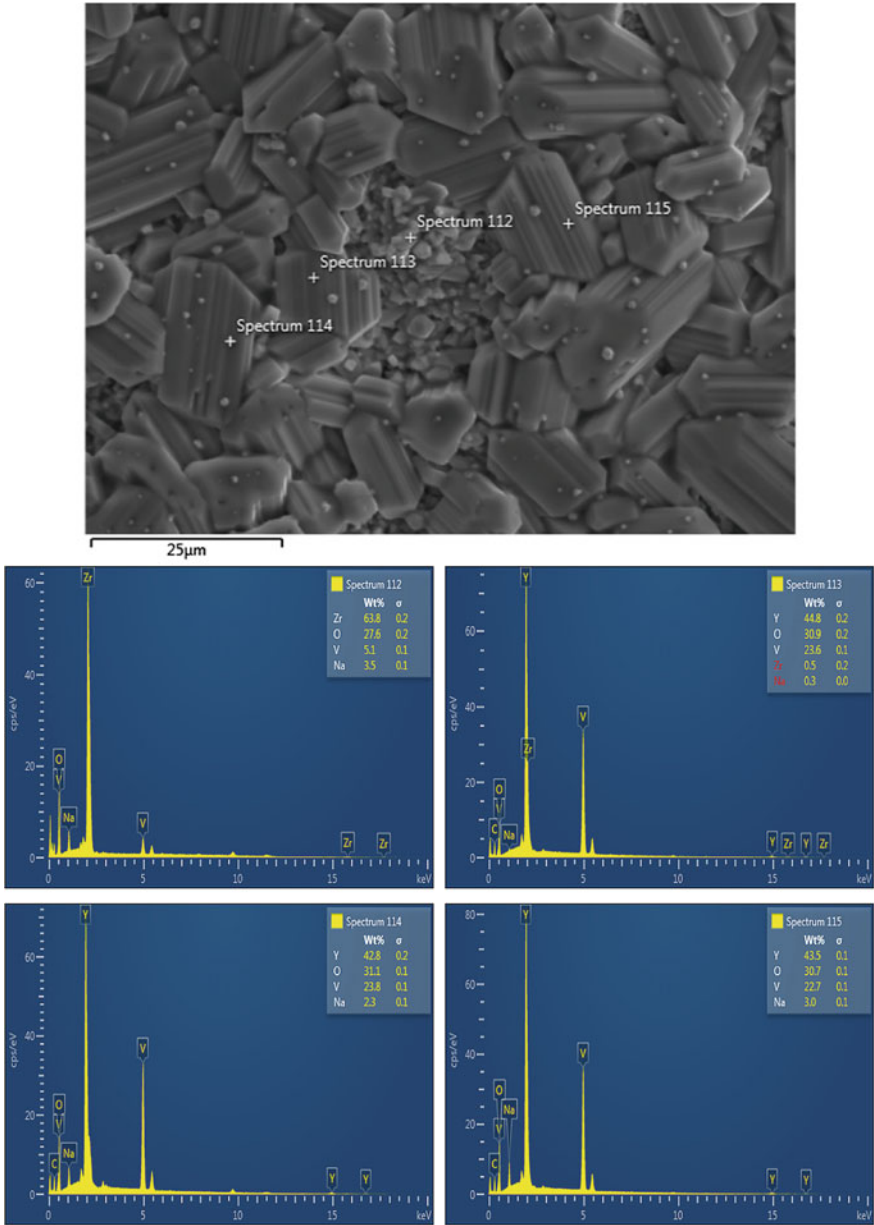


Fig. 12 Surface micrograph with EDS analysis of YSZ TBC produced by APS method with HVOF CoNiCrAlY bond coat after the hot corrosion test

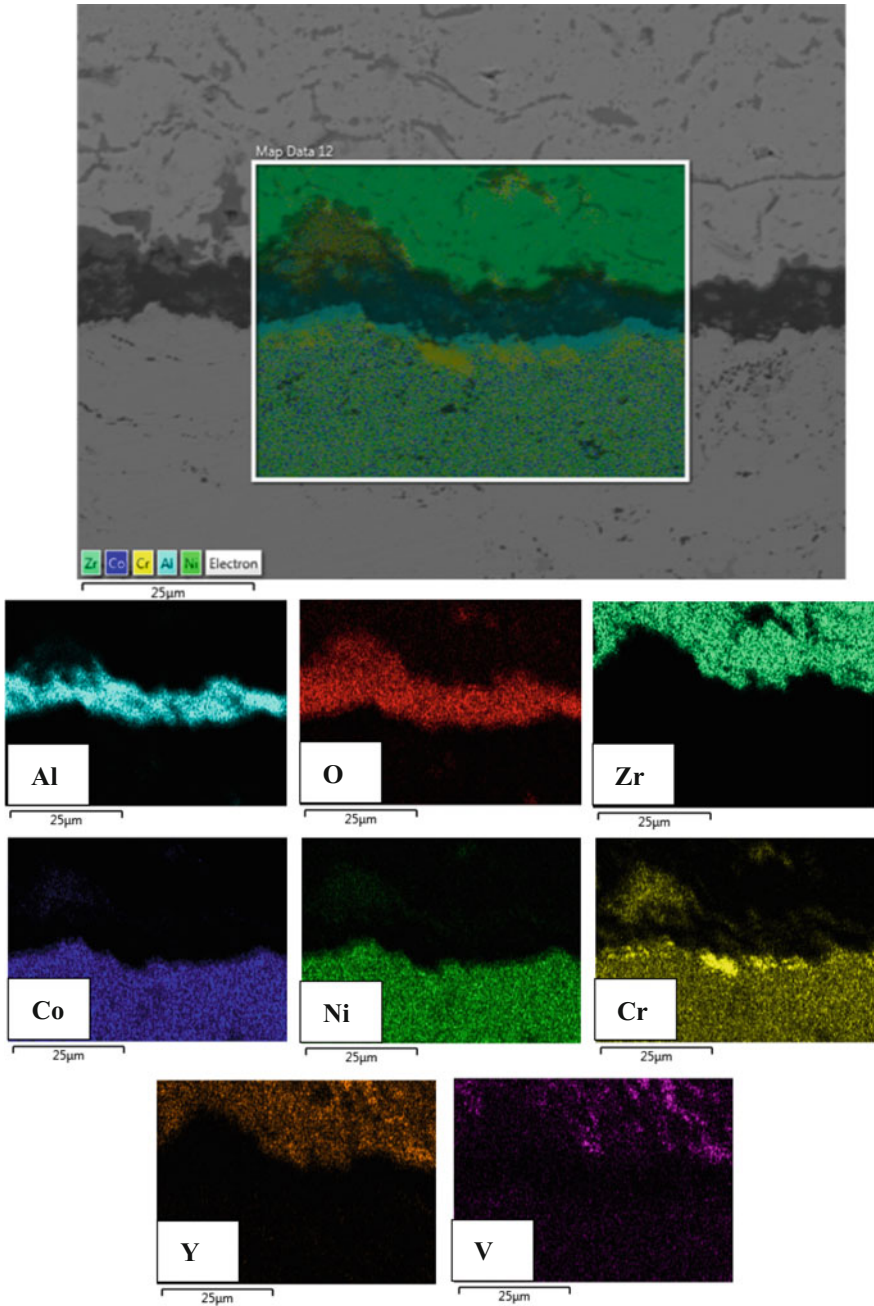


Fig. 13 Cross-sectional micrograph with elemental mapping analysis of YSZ TBC produced by APS method with HVOF CoNiCrAlY bond coat after the hot corrosion test

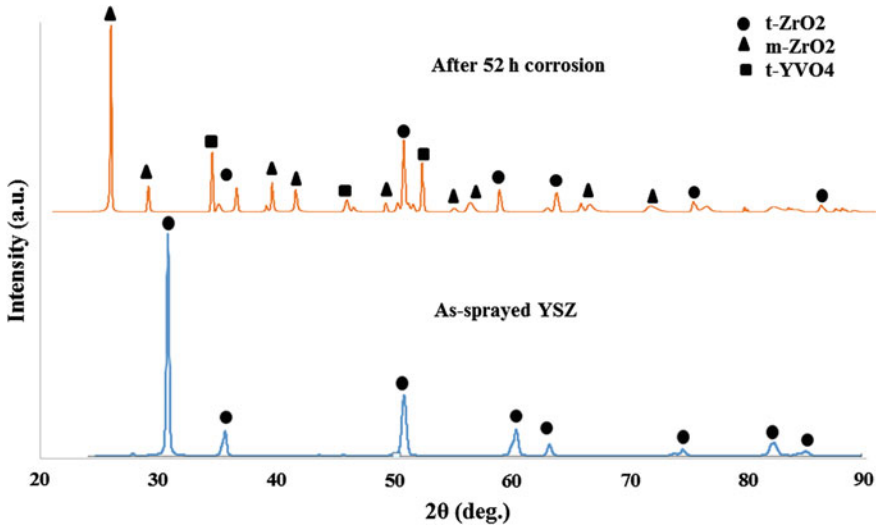


Fig. 14 XRD analysis of HVOF and CoNiCrAlY bond coat produced by APS before and after hot corrosion tests

1. The TBC system produced using the APS technique was found to have high porosity and oxide content whereas the one produced with HVOF technique had low porosity and oxide content.
2. Hot corrosion and failure of the YSZ coating was primarily because of molten corrosive salt containing V₂O₅ and Na₂SO₄.
3. The phases of m-ZrO₂ and YVO₄ crystals promoted crack formation and failure of TBCs. Thus, the molten salt mixture penetrated into the bond coat from cracks and open porosities on the surface of the coating, causing damage. At the same time, the elemental mapping analyses indicate that the molten salts penetrated through cracks.
4. The hot corrosion lifetime of the HVOF-BC system is higher than APS-BC. In addition, the formation rate of APS BC system was faster than that of HVOF BC at interface area with the TGO formation.

Acknowledgements The present study was derived from Ph.D. thesis of Mustafa Kaplan in the University of Selcuk Graduate School of Natural and Applied Sciences, Konya, Turkey. The study was also supported by Selcuk University Scientific Research Projects under the Grant Number of 15201071.

References

1. Sreedhar, G., Raja, V.S.: Hot corrosion of YSZ/Al₂O₃ dispersed NiCrAlY plasma-sprayed coatings in Na₂SO₄-10 wt.% NaCl melt. *Corros. Sci.* **52**, 2592–2602 (2010)

2. Heverana, C.M., Xua, J.P., Sarina, V.K., et al.: Simulation of stresses in TBC–EBC coating systems for ceramic components in gas turbines. *Surf. Coat. Technol.* **235**, 354–360 (2013)
3. Miller, R.A.: Thermal barrier coatings for aircraft engines: history and directions. *J. Therm. Spray Technol.* **6**, 35–42 (1997)
4. Karaoglanli, A.C., Doleker, K.M., Ozgurluk, Y.: State of the art thermal barrier coating (TBC) materials and TBC failure mechanisms. In: Ochner, A., Altenbach, H. (eds.) *Properties and Characterization of Modern Materials*. Springer, Germany (2017)
5. Liu, H.F., Xiong, X., Li, X.B., et al.: Hot corrosion behavior of Sc_2O_3 - Y_2O_3 - ZrO_2 thermal barrier coatings in presence of $\text{Na}_2\text{SO}_4 + \text{V}_2\text{O}_5$ molten salt. *Corros. Sci.* **85**, 87–93 (2014)
6. Karaoglanli, A.C., Turk, A.: Isothermal oxidation behavior and kinetics of thermal barrier coatings produced by cold gas dynamic spray technique. *Surf. Coat. Technol.* **318**, 72–81 (2017)
7. Ghosh, S.: Thermal barrier ceramic coatings—a review. In: Mohamed, A. (ed.) *Advanced Ceramic Processing*. InTech, London (2015)
8. Karaoglanli, A.C., Oge, M., Doleker, K.M., et al.: Comparison of tribological properties of HVOF sprayed coatings with different composition. *Surf. Coat. Technol.* **318**, 299–308 (2017)
9. Hajizadeh-Oghaz, M., Razavi, R.S., Ghasemi, A., et al.: Na_2SO_4 and V_2O_5 molten salts corrosion resistance of plasma-sprayed nanostructured ceria and yttria co-stabilized zirconia thermal barrier coatings. *Ceram. Int.* **42**, 5433–5446 (2016)
10. Li, S., Liu, Z.G., Ouyang, J.H.: Study on hot corrosion reactions between $\text{SmYbZr}_2\text{O}_7$ ceramic and vanadium pentoxide at temperatures of 600–1000 °C in air. *Mater. Chem. Phys.* **130**, 1134–1138 (2011)
11. Liu, L., Xu, H., Xiao, J., et al.: Effect of heat treatment on structure and property evolutions of atmospheric plasma sprayed NiCrBSi coatings. *Surf. Coat. Technol.* **325**, 548–554 (2017)
12. Aghasibeig, M., Moreau, C., Dolatabadi, A., et al.: Fabrication of nickel electrode coatings by combination of atmospheric and suspension plasma spray processes. *Surf. Coat. Technol.* **285**, 68–76 (2016)
13. Ajay, A., Raja, V.S., Sivakumar, G., et al.: Hot corrosion behavior of solution precursor and atmospheric plasma sprayed thermal barrier coatings. *Corros. Sci.* **98**, 271–279 (2015)
14. Tao, C., Wang, L., Cheng, N.L., et al.: Hot corrosion performance of $\text{AlO-CrO/NiCoCrAlYTa}$ and AlO/NiCoCrAlYTa coatings deposited by atmospheric plasma spraying. *J. Therm. Spray Technol.* **25**, 797–805 (2016)
15. Wang, L., Liu, C.G., Zhong, X.H., et al.: Investigation of crack propagation behavior of atmospheric plasma-sprayed thermal barrier coatings under uniaxial tension using the acoustic emission technique. *J. Therm. Spray Technol.* **24**, 296–308 (2015)
16. Saremi, M., Valefi, Z., Abaeian, N.: Hot corrosion, high temperature oxidation and thermal shock behavior of nano agglomerated YSZ-Alumina composite coatings produced by plasma spray method. *Surf. Coat. Technol.* **221**, 133–141 (2013)
17. Guo, L., Zhang, C.L., Li, M.Z., et al.: Hot corrosion evaluation of Gd_2O_3 - Yb_2O_3 co-doped Y_2O_3 stabilized ZrO_2 thermal barrier oxides exposed to $\text{Na}_2\text{SO}_4 + \text{V}_2\text{O}_5$ molten salt. *Ceram. Int.* **43**, 2780–2785 (2017)
18. Mohan, P., Yuan, B., Patterson, T., et al.: Degradation of yttria-stabilized zirconia thermal barrier coatings by vanadium pentoxide, phosphorous pentoxide, and sodium sulfate. *J. Am. Ceram. Soc.* **90**, 3601–3607 (2007)
19. Afrasiabi, A., Saremi, M., Kobayashi, A.: A comparative study on hot corrosion resistance of three types of thermal barrier coatings: YSZ, YSZ + Al_2O_3 and YSZ/ Al_2O_3 . *Mater. Sci. Eng. A* **478**, 264–269 (2008)
20. Sidhu, T.S., Prakash, S., Agrawal, R.D.: Hot corrosion performance of a NiCr coated Ni-based alloy. *Scripta Mater.* **55**, 179–182 (2006)
21. Ahmadi-Pidani, R., Shoja-Razavi, R., Mozafarinia, R., et al.: Evaluation of hot corrosion behavior of plasma sprayed ceria and yttria stabilized zirconia thermal barrier coatings in the presence of $\text{Na}_2\text{SO}_4 + \text{V}_2\text{O}_5$ molten salt. *Ceram. Int.* **38**, 6613–6620 (2012)
22. Wang, X.Z., Guo, L., Peng, H., et al.: Hot-corrosion behavior of a $\text{La}_2\text{Ce}_2\text{O}_7$ /YSZ thermal barrier coating exposed to $\text{Na}_2\text{SO}_4 + \text{V}_2\text{O}_5$ or V_2O_5 salt at 900 °C. *Ceram. Int.* **41**, 6604–6609 (2015)

23. Li, S., Liu, Z.G., Ouyang, J.H.: Hot corrosion behaviour of $\text{Yb}_2\text{Zr}_2\text{O}_7$ ceramic coated with V_2O_5 at temperatures of 600–800 °C in air. *Corros. Sci.* **52**, 3568–3572 (2010)
24. Loghman-Estarki, M.R., Razavi, R.S., Edris, H., et al.: Comparison of hot corrosion behavior of nanostructured ScYSZ and YSZ thermal barrier coatings. *Ceram. Int.* **42**, 7432–7439 (2016)
25. Li, M.Z., Cheng, Y.X., Guo, L., et al.: Preparation of plasma sprayed nanostructured GdPO_4 thermal barrier coating and its hot corrosion behavior in molten salts. *Ceram. Int.* **43**, 7797–7803 (2017)
26. Guo, L., Li, M.Z., Ye, F.X.: Comparison of hot corrosion resistance of $\text{Sm}_2\text{Zr}_2\text{O}_7$ and $(\text{Sm}_{0.5}\text{Sc}_{0.5})_2\text{Zr}_2\text{O}_7$ ceramics in $\text{Na}_2\text{SO}_4 + \text{V}_2\text{O}_5$ molten salt. *Ceram. Int.* **42**, 13849–13854 (2016)
27. Ramachandran, C.S., Balasubramanian, V., Ananthapadmanabhan, P.V.: On the cyclic hot corrosion behaviour of atmospheric plasma sprayed lanthanum zirconate based coatings in contact with a mixture of sodium sulphate and vanadate salts: a comparison with the traditional YSZ duplex and NiCrAlY coated samples. *Vacuum* **97**, 81–95 (2013)
28. Daroonparvar, M., Yajid, M.A.M., Yusof, N.M., et al.: Investigation of three steps of hot corrosion process in Y_2O_3 stabilized ZrO_2 coatings including nano zones. *J Rare Earth* **32**, 989–1002 (2014)